2012

Simulation of single polymer chains with influences of solid walls under imposed flow fields

Wenli Ouyang
Lehigh University

Simulation of single polymer chains with influences of solid walls under imposed flow fields

by

Wenli Ouyang

A Thesis

Presented to the Graduate and Research Committee

of Lehigh University

in Candidacy for the Degree of

Master of Sciences

in

Mechanical Engineering

Lehigh University

Thesis is accepted and approved in partial fulfillment of the requirements for the Master of Science in Mechanical Engineering.

Simulation of single polymer chains with influences of solid walls under imposed flow fields
Wenli Ouyang

_____

Date Approved

_____

Thesis Advisor

_____

(Name of Co-Advisor)

_____

(Name of Department Chair)

ACKNOWLEDGMENTS

I would like to take this time to express my sincere gratitude and appreciation to everyone who contributed to this research. Firstly, I'd like to thank all of my advisors, Dr. Alparsian Oztekin; Dr. Edmund Webb III and Dr. Frank Zhang, for their extensive guidance and assistance during the past one year. It would have been impossible for me to finish this research without their continuous support and encouragement.

Thank Wei Wei for discussing research with me, helping me understanding models and FORTRAN programming. I also would like to thank Haolin Ma for his suggestions and instructions. And I'd like to thank all my colleagues and friends at Lehigh University, who provided continuous encouragement and support during my study at Lehigh.

TABLE OF CONTENTS

LIST OF FIGURES

ABSTRACT

The interactions between a single polymer chain and a solid wall are studied in the presence of the specific shear flow field. Coarse-grained Brownian molecular dynamic simulations have been carried out to study the effects of wall on the conformational changes of a single polymer chains under various shear flow conditions. The Polymer chain is modeled by a sequence of 20 beads connected by finitely extensible non-linear elastic springs. The results show that the strongly attractive solid wall will pull the polymer chain towards it, compared with the weakly attractive solid wall that pushes the polymer chain away. When the polymer chain sticks to the wall and flow field is strong enough, it unfolds significantly. It is also shown that the initial distance between the wall and the polymer chain has little influences on the configuration of the polymer chain near weakly attractive walls. On the other hand, the initial distance has strong influences on the dynamics of polymer chain near strongly attractive walls. Our prediction indicates that there is a critical value of shear rate for a polymer chain near strongly attractive walls. For the value of shear rate above the critical value, the polymer chain unfolds significantly.

Chapter 1. Introduction

The interaction between polymer chains and solid walls has attracted great attentions recently. The dynamic behavior of the polymer chains near surfaces can be important in several technological applications such as microelectronics, colloidal stability, surface nanopatterning, adhesion, and friction modification.[1] The present work uses Brownian Dynamic simulations to examine the configuration of simple polymer chains under the influence of solid walls.

Brownian Dynamic simulation is a well-accepted tool to be used study polymer and molecular systems. Brownian Dynamics is a limiting case of Langevin dynamics and it can be used for systems in which inertial effects are negligible. Starkweather et al. (1998) studied single-chain entanglements in dilute solution capillary electrophoresis. The Monte Carlo simulation procedure used by these investigators employs a pearl necklace representation of the polymer chain, and each bead in the chain is given a hard sphere potential and radius large enough to prevent crossings. Saville and Sevick (1999) study a field-driven polymer chain colliding with a finite-sized obstacle. They discuss the "unhooking" and "rolling off" mechanisms for chain release. Nixon and Slater (1994) use bead-rod Brownian dynamics to simulate two-dimensional DNA electrophoretic collisions with a single non-moving obstacle.[2]

However, due to computational limitations, these simulation methods can only be used to simulate either shorter chains (a hundred monomers) or longer

chains for a shorter time scale (at most microseconds).[3] In order to simulate practical situations where long polymers and span time scales of the order of seconds, BD simulation of bead-spring chains has been utilized. In the model, the polymer chain is represented by a sequence of beads connected by flexible springs where the beads act as drag centers and they interact with each other via various forces that will be mentioned next chapter. Specifically, the model that is proposed by Kumar and Larson is used in the present work. The model will be presented in detail in Chapter 3.

The main objective of the thesis is to examine the effect of the wall on the conformational changes of a polymer chain. The wall is modeled as an infinite impenetrable solid boundary, which determines the molecules are unable to travel through it. The parameter ε_{wall} that determines the attractive capability of the wall can be properly chosen to study both strongly attractive and weakly attractive walls. Conformational changes of the polymer chain is characterized by two parameters Rg and Rz determined by the simulation. Rg is the radius-of-gyration of the polymer chain and Rz is the average distance between the centers of the each bead to the wall.

The flow induced conformational changes of a polymer chain near a wall is investigated. Only simple shear flow is considered in the present work. Using different energy parameters of bead-wall interactions and the static and dynamic properties of a polymer chain are investigated for various shear flow conditions.

The thesis is outlined as follows. Chapter Two describes Bead-Spring model; Brownian Dynamics; Wall effect and briefly reviews the past studies.

Chapter Three describes the mathematical model; Chapter Four describes the numerical method. In Chapter Five, the results are presented and discussed. The conclusion is presented in Chapters Six.

Chapter 2. Literature Review

2.1 Bead-Spring Model

The bead-spring model is a model simulating the hydrodynamic properties of a chain macromolecule consisting of a sequence of beads, each of which offers hydrodynamic resistance to the flow of the surrounding medium and is connected to the next bead by a spring which does not contribute to the frictional interaction. The spring is responsible for the elastic and deformational properties of the chain. And mutual orientation of the springs is random.[4]

The idea of bead-spring model can trace back to more than 60 years ago and consists of many submodels. The Rouse model was proposed by Prince E. Rouse in 1953. The Rouse describes the conformational dynamics of an ideal chain. In this model, the single chain diffusion is represented by Brownian motion of beads connected by harmonic springs (Hookean). There are no excluded volume interactions between the beads and each bead is subjected to a random thermal force and a drag force as in Langevin dynamics.[5] The linear force law used in the Rouse model has the advantage that it greatly simplifies the mathematics and allows a number of equilibrium and nonequilibrium properties. The Rouse model is expressed by an explicit constitutive equation. However the linear force law leads to unrealistic results when the chain is subjected to large deformations, presumably because the chain can be extended infinitely.[6] one important extension to the model is the hydrodynamic interactions mediated by

the solvent between different parts of the chain introduced out by Bruno Zimm.[7] Whilst the Rouse model overestimates the decrease of the diffusion coefficient D with the number of beads N as $1/N$, the Zimm model predicts $D \sim 1/N^{v}$ which is consistent with the experimental data for dilute polymer solutions. But the Zimm model has the similar issue as the Rouse model that is only realistic for small deformations from equilibrium and put no limit to the extent to which the spring can be stretched. Thus the deficiencies of models with Hookean springs have led investigators to shift their attention to models based on a bead-spring chain with finitely extensible nonlinear elastic (FENE) spring.[6]

The bead-spring model with FENE spring has been widely researched and used after its first debut. Warner[8] computed perturbation solutions and numerical solutions for steady shear flow. Armstrong[9] obtained perturbation solutions for an arbitrary non-linear elastic spring force in steady homogeneous flow and in the linear viscoelastic limit. Christiansen and Bird[10] extrapolated a perturbation solution also for high amplitude oscillatory shear flow. More recently, Fan[11] improved Warner's numerical method.

In the present work, the bead-spring model where N beads connected to the neighboring beads by FENE springs will be used. The finitely extensible nonlinear elastic spring law[12] is employed

$$\mathbf{F}_{spring} = \frac{\mathbf{Q}}{1-\mathbf{Q}^2/b} \tag{1}$$

The detailed description of the spring law is given in Chapter 3.

2.2 Brownian Dynamics (BD) Simulation

The Brownian Dynamics is a simplified version of Langevin dynamics, in which the average acceleration can be neglected. So BD is also named non-inertial dynamics. Briefly, Langevin dynamics uses a stochastic differential equation in which two force terms have been added to Newton's second law. Since a molecule in the real world is not present in a vacuum and solvent molecules causes friction and collisions to perturb the system. For a system of N particles with masses M, with coordinates $X = X(t)$ that constitute a time-dependent random variable, the resulting Langevin equation is given in the form:

$$M\ddot{X}(t) = -\nabla U(X) - \gamma M\dot{X}(t) + \sqrt{2\gamma k_B TM}\,R(t) \tag{2}$$

Since Brownian dynamics is inertial dynamic. The $M\ddot{X}(t)$ term is neglected. The equation governing the Brownian dynamic is:

$$0 = -\nabla U(X) - \gamma M\dot{X}(t) + \sqrt{2\gamma k_B TM}\,R(t) \tag{3}$$

In equation (3), $U(X)$ is the particle interaction potential; k_B is the Boltzmann's constant; $R(t)$ is a delta-correlated Gaussian process with zero-mean and γ

represent the collision frequency that controls the magnitude of the frictional force and the variance of the random forces.

The BD simulation, an extremely efficient method for treating molecular, is proposed as early as 1978 by D.L. Ermak and J.A. McCammon.[13] They present BD simulations of short chains with hydrodynamic interaction (HI) at equilibrium. Almost at the same time, Fixman[14] developed and applied the mathematical background for performing BD simulations of polymer chains in flow. BD simulations of FENE dumbbell models with HI and excluded volume (EV) effects were simulated by Rudisill and Cummings.[15] The rheological properties of FENE chains, in comparison with various approximations, have been investigated via BD simulation by van den Brule.[16] More recently, J.S. Hur and R.G. Larson simulated single DNA molecules in shear flow using BD simulations and the simulation results, especially in light of the excellent agreement with experiment, demonstrated the basic physical elements necessary for any rheological model to capture the dynamics of single polymer chains in flow.[17] Later M. Chopra and R.G. Larson extended the BD simulations into isolated polymer molecules in shear flow near adsorbing and nonadsorbing surfaces.[18]

The molecular dynamic simulation is the method used by the present work. Specific of the method are described in Chapter 3.

2.3 The Wall Effect

The wall effect towards the behavior of polymer solutions has received a great deal of attention in the past three decades, not only because of its intrinsic scientific interest but also because of its technological importance.[19] In the existing studies of the wall effect, De Gennes[20,21], J.M.H.M. Scheutjens[22] and H.J. Ploehn[23] have focused on the equilibrium (static) problem while J.H. Aubert[24] and P.O. Brunn[25] have undertaken the same problem under flow conditions on the contrary. During that period, a fairly good understanding has been developed.

More recently, Duering and Rabin[26] and de Pablo et al[27] have applied two-dimensional Monte Carlo and other stochastic methods in computer simulations of rigid dumbbells and multi-bead-rod models with impacts of the wall effect. Mavrantzas and Beris[28] have developed the Hamiltonian formalism for flowing polymers near surfaces.

Remarkably, S.W. Sides and G.S. Grest have conducted large-scale simulations of adhesion dynamics for end-grafted polymer.[29] Later they have simulated the effect of end-tethered polymers on surface adhesion of glassy polymers.[30] They utilized an effective 9-3 Lennard-Jones potential that is an integrated form of standard LJ potential, which describes impacts of infinitely flat wall towards polymer chains.

$$\mathbf{F}_i^{BW} = \frac{4}{d^{ev}}[9(\frac{d^{ev}}{z_i})^{10} - 3\varepsilon_{wall}(\frac{d^{ev}}{z_i})^4]\mathbf{z} \qquad (4)$$

where **z** is the unit vector in the z direction and z_i is the distance between the center-of-mass of the bead and the wall. And ε_{wall} and d^{ev} are energy and length parameters of bead-wall, respectively. The detailed description of this method is given in Chapter 3.

Chapter 3. Model Descriptions

3.1 Physical forces

For the Bead-Spring Model, the following physical forces are of the real importance.

3.1.1 Brownian force

When a polymer chain is suspended in a fluid, each bead subjected to the impact of liquid molecules. For ultra-fine beads, the instantaneous momentum imparted to beads varies random that causes beads to move on an erotic path now known as Brownian motion. The Brownian force is given by:

$$\mathbf{F}_{Brownian} = (\frac{6k_B T\zeta}{\Delta t})^{1/2} \tag{5}$$

where k_B is the Boltzmann's constant, T is the absolute temperature, ζ is the drag coefficient for a bead, and Δt is the time-step used in the simulation.

3.1.2 Spring force

The spring forces are caused by flexible springs used to connect beads in a polymer chain sequentially. And the dimensionless spring forces $\mathbf{F}_{spring}$ are able to calculate by a finitely extensible nonlinear elastic law (Bird et al. 1987):

$$\mathbf{F}_{spring} = \frac{\mathbf{Q}}{1-\mathbf{Q}^2 / b} \tag{6}$$

where $\mathbf{Q} = \mathbf{r}_{i+1} - \mathbf{r}_i$. The flexibility of a spring is measured by the dimensionless extensibility parameter b and is defined as:

$$b = HQ_0^2 / k_B T = 3N_{K,s} \tag{7}$$

where $N_{K,s}$ is the number of Kuhn steps in a spring and Q_0 is the length of a fully extended spring.

3.1.3 Viscous drag force

The viscous drag is the frictional force that the flowing solvent exerts on polymer chains that how an important influence on the configurations of polymer chains. The viscous drag force is given by:

$$\mathbf{F}_i^{HI} = \zeta(\mathbf{V}_i - \dot{\mathbf{r}}_i) \tag{8}$$

where ζ is the drag coefficient too, $\mathbf{V}$ is the bulk velocity of the solvent at the bead location, and $\dot{\mathbf{r}}$ is the velocity of the bead $\dot{\mathbf{r}} = d\mathbf{r}/dt$.

3.1.4 Bead-bead Lennard-Jones potential

The Lennard-Jones potential is a special case of Mie potential. It consists of two parts: a steep repulsive term and a smoother attractive term. It is worth mentioning that the 12-6 Lennard-Jones potential model is not the best representation of the potential energy surface, but rather its use is widespread due to its computational expediency. A truncated Lennard-Jones potential is used here to model bead-bead interactions:

$$F_{i,j}^{BB} = \frac{4}{d^{ev}}[12(\frac{d^{ev}}{r_{ij}})^{13} - 6\varepsilon(\frac{d^{ev}}{r_{ij}})7]r_{ij} \text{ for } r_{ij} \geq 0.675 \tag{9}$$

$$F_{i,j}^{BB} = \frac{4}{d^{ev}}[12(\frac{d^{ev}}{r_{ij}})^{13} - 6\varepsilon(\frac{d^{ev}}{r_{ij}})7]r_{ij} \text{ for } r_{ij} \leq 0.675 \tag{10}$$

where $\mathbf{r}_{ij}$ is the unit vector along $\mathbf{r}_{ij}$, and ε and d_{ε}^{ev} are the energy and length parameters of bead-bead interactions, respectively.

The Lennard-Jones potential acting on a bead due to bead-bead interactions thus can be written in the form:

$$\mathbf{F}_i^{BB} = \sum_{j \neq i} \mathbf{F}_{i,j}^{BB} \tag{11}$$

3.1.5 Bead-wall Lennard-Jones potential

The interactions between an infinite flat wall and the polymer beads are modeled by an integrated 9-3 lennard Jones potential. The 9-3 Lennard-Jones potential is commonly used to model the interaction between the molecules of a fluid with a structureless solid wall. The potential force is expressed as:

$$\mathbf{F}_i^{BW} = \frac{4}{d^{ev}}[9(\frac{d^{ev}}{z_i})^{10} - 3\varepsilon_{wall}(\frac{d^{ev}}{z_i})^4]\mathbf{z} \tag{12}$$

where $\mathbf{z}$ is the unit vector in the direction normal to the wall, z_i is the distance between the center-of-mass of the bead and the wall, and ε_{wall} and d^{ev} are energy and length parameters of bead-wall, respectively.

The effects of the weakly attractive wall and strongly attractive wall can be examined by choosing ε_{wall} properly. ε_{wall} <<0.1 to simulate weakly attractive walls while ε_{wall} >> 1 to simulate the strongly attractive wall. And we get the graphs about the bead-wall LJ potential force versus z_i as below.

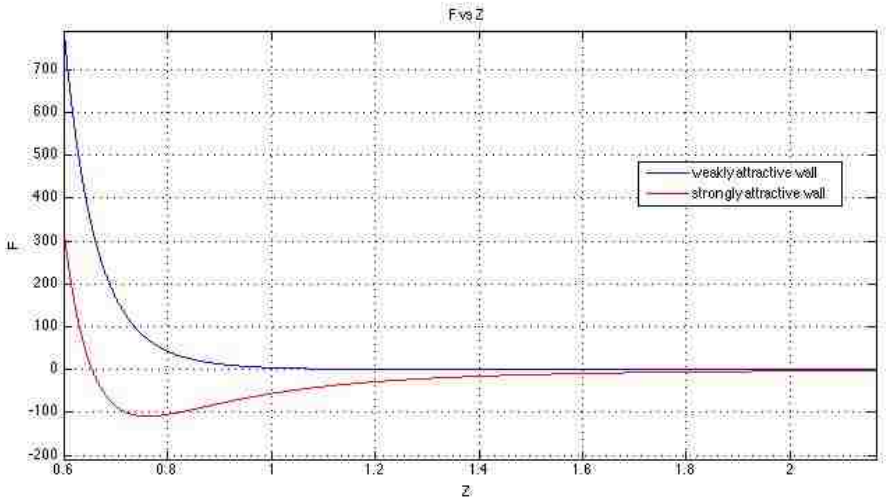

Figure 1 (a) the bead-wall LJ potential forces as a function of the distance between the center of mass of the beads and the wall for ε_{wall} = 0.1 and 10.

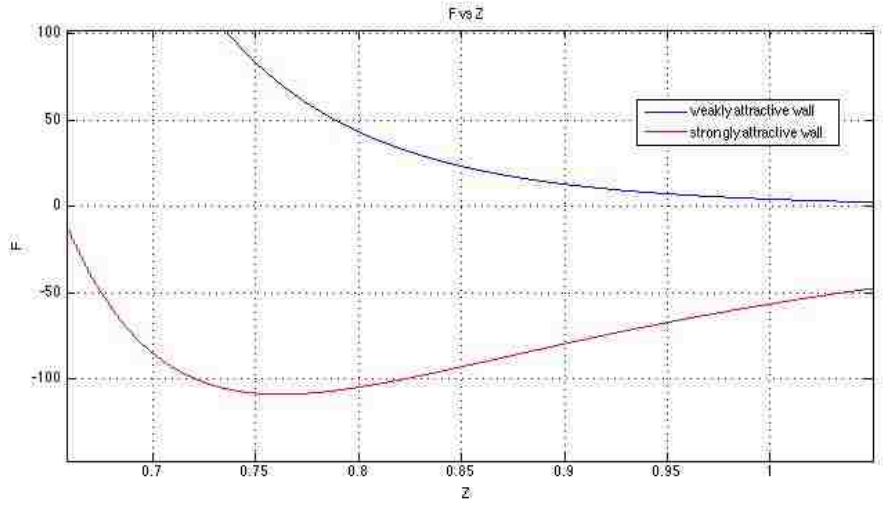

Figure 1 (b) the bead-wall LJ potential forces as a function of the distance between the center of mass of the beads and the wall for when ε_{wall} = 0.1 and 10 for 0.65<z<1.05.

3.2 Governing equations

The BD methods take advantage of the fact that inertial forces on the polymers are small, and therefore, the sum of the above forces can be set to zero:

$$F_i^{HI} + F_i^S + F_i^{BB} + F_i^{BW} + F_i^B = 0 \text{ for } i = 1, 2, ..., N \tag{13}$$

Substituting equations (5) ~ (12) into the force balance equation yields:

$$-\zeta\left[\frac{\mathbf{r}_i - \mathbf{r}_i^{old}}{\Delta t} - (\nabla \mathbf{u})^T \cdot \mathbf{r}_i\right] + F_i^S - F_{i-1}^S + F_i^{BB} + F_i^{BW} + \sqrt{\frac{6k_bT}{\zeta \cdot \Delta t}}\mathbf{n}_i = 0 \tag{14}$$

Measuring length in units of $\sqrt{k_BT/H}$, force in units of $\sqrt{Hk_{\mathbf{B}}T}$ and time in units of ζ / H, the dimensionless equation governing the conformational changes of polymer can be written in the form (Bird er al. 1987):

$$\mathbf{r}_i = \mathbf{r}_i^{old} + \left[(\nabla \mathbf{u})^T \cdot \mathbf{r}_i + \mathbf{F}_i^S - \mathbf{F}_{i-1}^S + \mathbf{F}_i^{BB} + \mathbf{F}_i^{BW}\right]\Delta t + \sqrt{2\Delta t}\mathbf{n}_i \tag{15}$$

where $\mathbf{r}_i$ and $\mathbf{r}_i^{old}$ are the position vectors of bead i at the new and old times, respectively, ∇ is the gradient operator, $\mathbf{u}$ is the unperturbed solvent velocity and $\mathbf{n}_i$ is the random vector whose components are uniformly distributed in $[-1,1]$, and Δt is the time-step used in the simulation.

3.3 Calculated Parameters

The results of the simulations are presented using two parameters.

3.3.1 The radius of gyration R_g

The radius-of-gyration (R_g) is used to characterize the conformation of a polymer chain and is defined by:

$$R_g = \sqrt{\frac{\sum_{i=1}^{N} \left| \mathbf{r}_i - \mathbf{r}_{c.m.} \right|^2}{N}} \tag{16}$$

where $\mathbf{r}_i = (x_i, y_i, z_i)$ is the position of the *ith* bead, and $\mathbf{r}_{c.m.} = (x_{c.m.}, y_{c.m.}, z_{c.m.})$ is the center of mass of the chain.

3.3.2 The distance between the polymer chain and the wall R_Z

The R_Z is used to characterize the relative position between the polymer chain and the wall. And it's written in the form:

$$R_Z = \frac{\sum_{i=1}^{N} \left| z_i - z_w \right|}{N} \tag{17}$$

where z_i is the shortest distance between the bead, and z_w is the position of the wall.

Chapter 4. Numerical Method

In this chapter, the numerical method using Brownian dynamics will be explained. The simulations were run on several Packer Lab 201 room's computers, with 16.0 gigabytes of memory, and 6 dual core i7 main processors and floating-point coprocessor running at 3.20 GHz. Each simulation took about 6 hours computational time. Numerical procedure is divided into two stages: initialization and the main simulation.

4.1 Initialization

Initialization is always the first part of the numerical procedure, and 25 random conformations of polymer chains and the walls are initialized at first and the properties of the polymer chain are estimated by averaging over these 25 random trajectories in order to reduce the unnecessary errors. The polymer chain has to stay on one side of the impenetrable wall. If the conformations don't satisfy above criteria, the initialization has to be done again until it meets the condition. Specifically, the initial chain conformations are generated by placing the first bead at the origin and the wall at a constant distance from it. Subsequent beads, $i = 2,3,.....,N$, are generated at random locations $\sqrt{3}$ (in dimensionless unites) away from the beads that precede them, see Fig. 2 (a) and Fig. 2(b). And importantly, four output files are created for each run in order to initial conditions

and calculated parameters. ‘initial.dat’ and ‘data.dat’ are used to record the initial positions and final positions of each bead while ‘Rg.dat’ and ‘Zg.dat’ are used to record the value of R_Z and R_Z of each time-step.

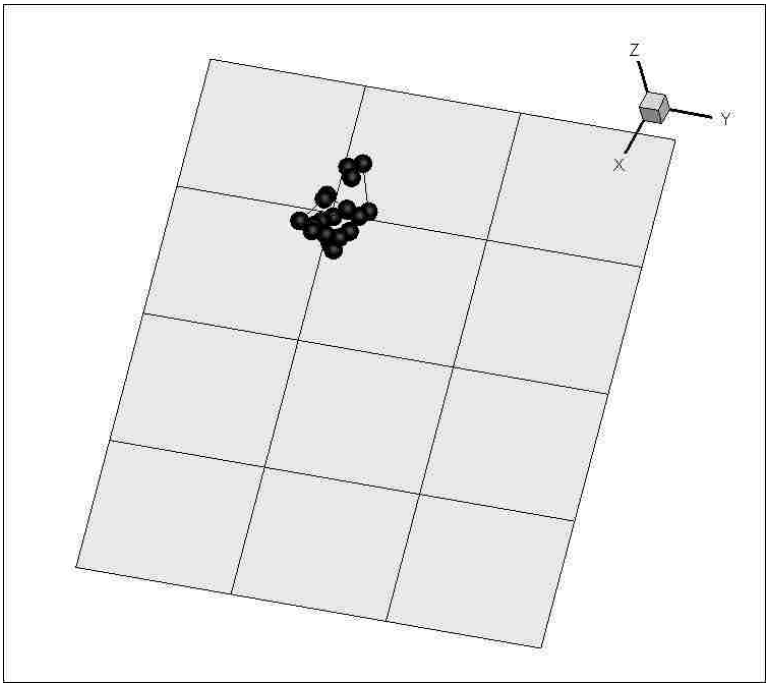

Figure 2 (a) Schematic representation of a single polymer chain confined by a solid wall (infinite) in initial position.

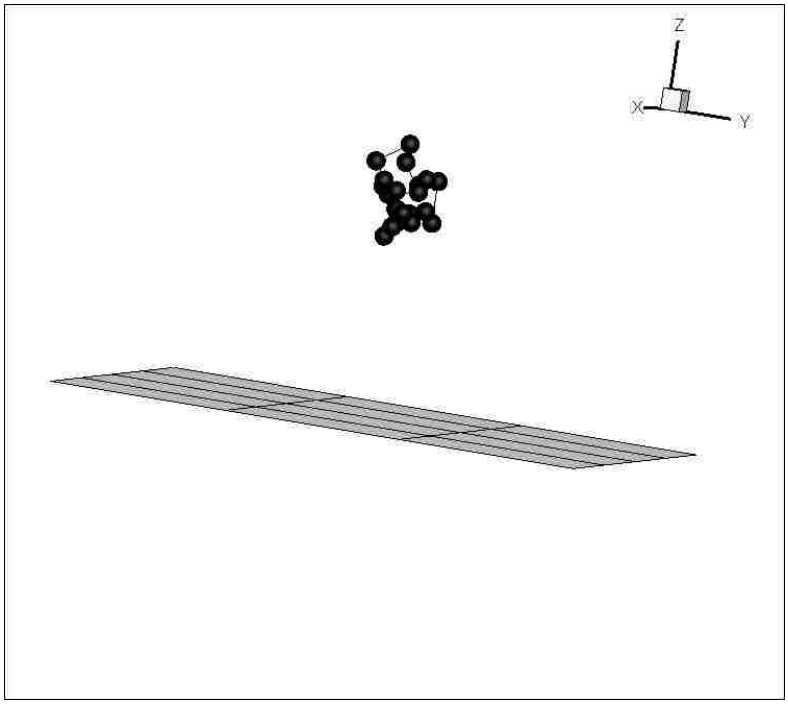

Figure 2 (b) Schematic representation of a single polymer chain confined by a solid wall (infinite) in initial position.

4.2 The main loop

The main loop of the program begins with calculation of forces influencing the movement of each bead. Specifically, the 'FENE.f90' subroutine is called to calculate spring forces; the 'Lennard_Jones.f90' subroutine is used to calculate the potential force between two different beads and the 'wallforce.f90' subroutine is called to calculate the wall-bead interactions. At first, the data of initial positions of beads are transferred from the initialization program to the subroutines. Then the specific forces are calculated and transferred back to the main program.

Next step is to calculate the conformational changes of polymer at various runs. The equations are solved using an explicit time-stepping algorithm. It is essentially marching in time; the position of each bead is determined using the position at past state. The radius of gyration (R_g) and the shortest distances of each bead from the wall (R_Z) are recorded at each time steps.

4.3 Parameters used in the numerical simulations

4.3.1 Time step

Because the low order of accuracy of the Brownian force term in the equation of motion of individual beads, small time steps must be used, even when the velocity gradient in the gap is small. For the majority of our simulations when there is no shear flow, the time-step Δt is set to be 1×10^{-4}. When the polymer chain in high shear flow, the time step size is $\Delta t \sim 1\times10^{-5}$. It should be noticed that there is a trade-off between accuracy and the total length of the simulation time.

4.3.2 Relaxation time and shear rate

The magnitude of shear flow is quantified by the Weissenberg number, which is defined as $Wi = \tau_{1,R}\dot{\gamma}$ where $\tau_{1,R}$ is the longest Rouse relaxation time of

polymer chain and $\dot{\gamma}$ is the rate of simple shear flow near the wall. The relaxation time of a chain connected by Hookean springs is given by[13] :

$$\tau_{1,R} = \frac{\zeta N_{K,s} b_K^2}{24 k_B T \sin^2(\pi / 2N)} = \frac{\zeta}{8H \sin^2(\pi / 2N)} \tag{18}$$

where b_K is the Kuhn step length, and the expression on the far left is obtained by using the relation, $H = 3k_B T / (N_{K,s} b_K^2)$. Notably, the presence of intramolecular interactions only slightly affects the relaxation dynamics. (Nazish Hoda, R.G. Larson, 2010) Using the method described above, here the relaxation time of a 20-bead chain (in units of ζ / H) for the model used here is 15.

4.3.3 Choice of length parameter and energy parameter

The energy parameter ε is the measure of how strongly the two beads attracted each other. For bead-bead interactions, the energy parameter ε_{bead} is fixed at 1. However the energy parameter of wall-bead interactions ε_{wall} is changing from 0.1 to 10 gradually in order to simulate a weakly attractive wall and a strongly attractive wall.

The length parameter d^{ev} gives a measurement of how close two nonbonding beads can get and is thus referred to as the van der Waals radius. It is equal to one-half of internuclear distance between nonbonding particles. Thus the

length parameter of bead-bead interactions and wall-bead interactions d^{ev} is all fixed at 0.8 according to the requirements of the simulation.[32]

Chapter 5. Results and Discussions

First, a simple test problem is considered, a single polymer chain in a quiescent solution confined by an impenetrable wall. In the absence of flow, the only external forces the molecule experiences are the Brownian kicks provided by the surrounding liquid, the viscous drag that resists the resulting movement of the molecule, the potential forces between the wall and the molecule. The conformational changes the molecule undergoes in the process are resisted by its entropic spring forces that are limited by its finite extensibility and Lennard-Jones potential forces that can be repulsive and attractive depending on distances between each molecule.

In the second set of more interesting problems, the conformational changes of a polymer chain near wall are studied under the influence of a simple shear flow. In addition to the random Brownian motion, the potential forces between different molecules and between the wall and each molecule, the spring forces, and the viscous drag, the polymer chain experiences the interactive force with the flow.

5.1 Quiescent solution

For the case of a quiescent liquid, one of the significant parameter in the simulation is the initial distance between the polymer chain and the wall. It is

characterized by z_{ini} as described above. The question is that to what extent, z_{ini} influences the configuration of the polymer chain. Simulations are conducted for various values of z_{ini} from 3 to 20.

The radius of gyration (R_g) for z_{ini}=10 and ε_{wall}=0.5 in the quiescent state of solvent as a function of time is plotted in Figure 3(a) and 3(b). For one of the 25 random set of initial beads configurations, the polymer chain reaches quasi-steady state quickly for any initial configuration set; namely R_g fluctuates around the mean value, as shown in Figures 3(a) and 3(b). For a given set of parameters and for the random initial configuration, the mean value of R_g is calculated. The radius of gyration (R_g) determined from each random initial configuration is then averaged ever as random initial configuration used for each run. The averaged value of R_g is then plotted against the wall energy parameter for various values of z_{ini}.

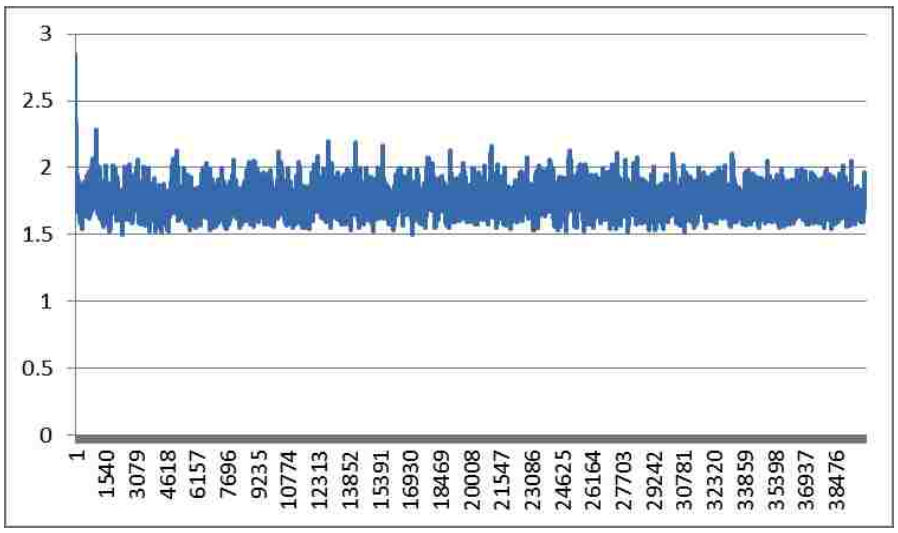

Figure 3 (a) the radius-of-gyration R_g versus time-steps in the case that z_{ini} =10 and ε_{wall} =0.5 in the quiescent state.

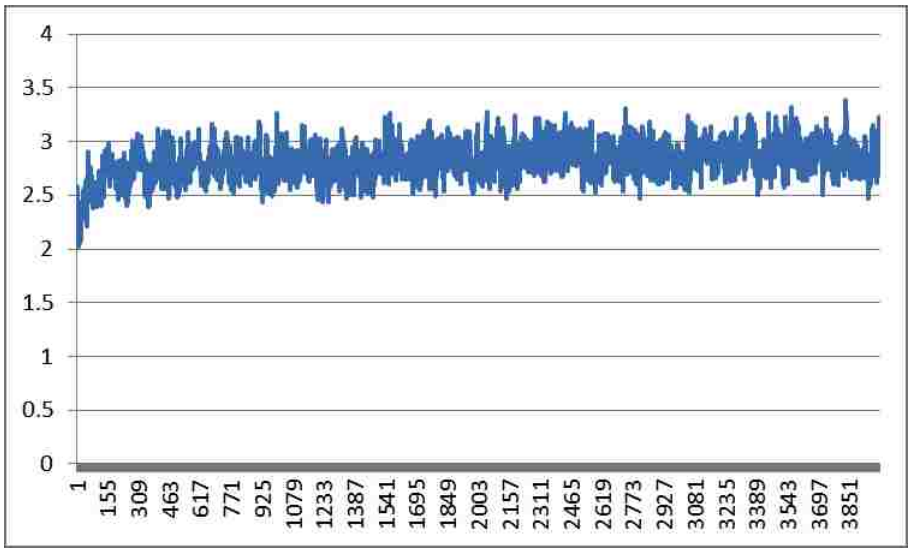

Figure 3 (b) the radius-of-gyration R_g versus time-steps in the case that z_{ini} =10 and ε_{wall} =5 in the quiescent state.

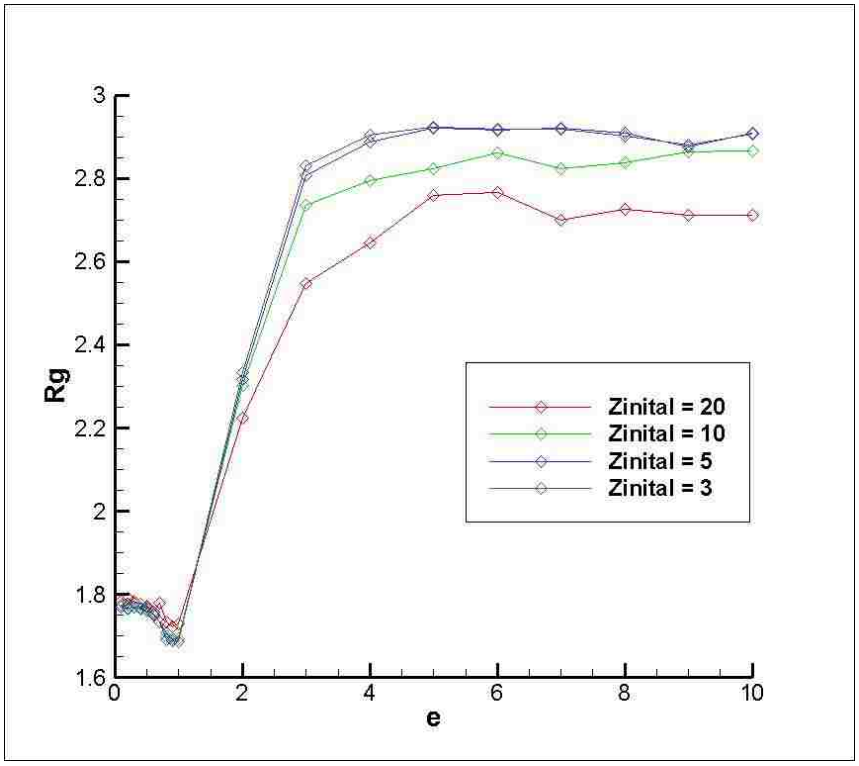

Figure 4 (a) Dependence of radius-of-gyration R_g on energy parameter of bead-wall interactions ε_{wall} in case when z_{ini}=20; z_{ini}=10; z_{ini}=5 and z_{ini}=3.

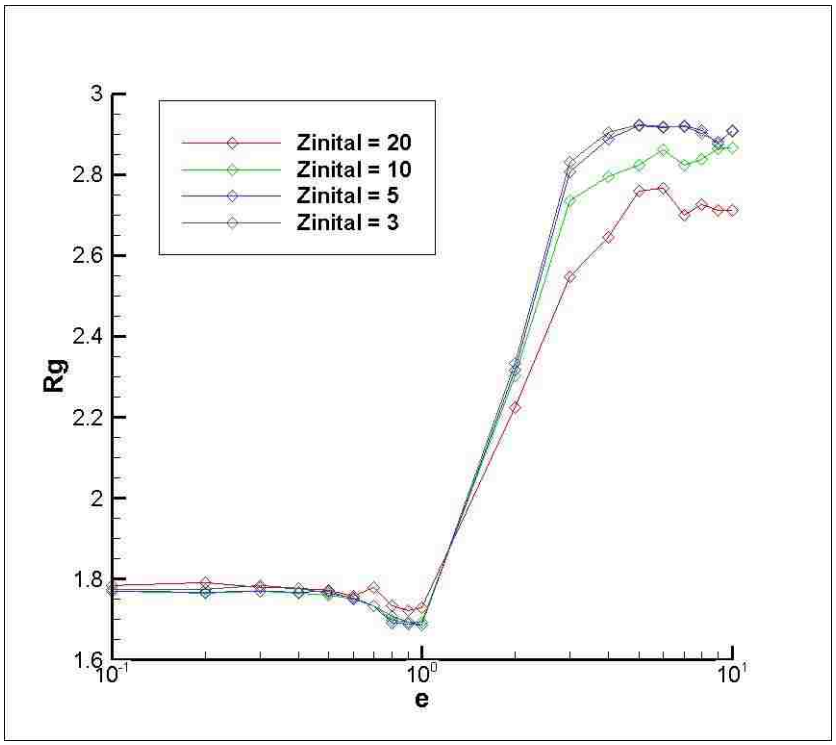

Figure 4 (b) Dependence of radius-of-gyration R_g on energy parameter of bead-wall interactions ε_{wall} in case when z_{ini}=20; z_{ini}=10; z_{ini}=5 and z_{ini}=3 and the value of ε_{wall} is using log scale.

It is noted that Figures. 4 (a) and (b) depict that the dependence of average value of radius-of-gyration R_g on the energy parameter ε_{wall} for the four cases when z_{ini} =20; z_{ini} =10; z_{ini} =5 and z_{ini} = 3. z_{ini} has profound effects on the configuration of the polymer chain. When $0 < \varepsilon_{wall} < 1$, the influence of z_{ini} on the dynamics of the polymer chain is not significant, as shown in Figures 4(a) and 4(b). This is due to the fact that for $0 < \varepsilon_{wall} < 1$, the attractive force is comparatively small. (See Figure 1(a) and (b)) And the polymer chain drifts away from the wall as shown in Figure 5(a). However for $1 < \varepsilon_{wall} < 4$, there is a clear transition, namely R_g increases rapidly as ε_{wall} increases. The polymer chain approaches to the wall as it unfolds, as shown in Figure 5(b). For $\varepsilon_{wall} > 4$, the effect of wall on the conformation of a polymer chain becomes noticeably obvious.

Figure 5 (a) the distance between the center of the polymer chain and the wall Rz versus time-steps in the case that z_{ini} =10 and ε_{wall} =0.4 in the quiescent state.

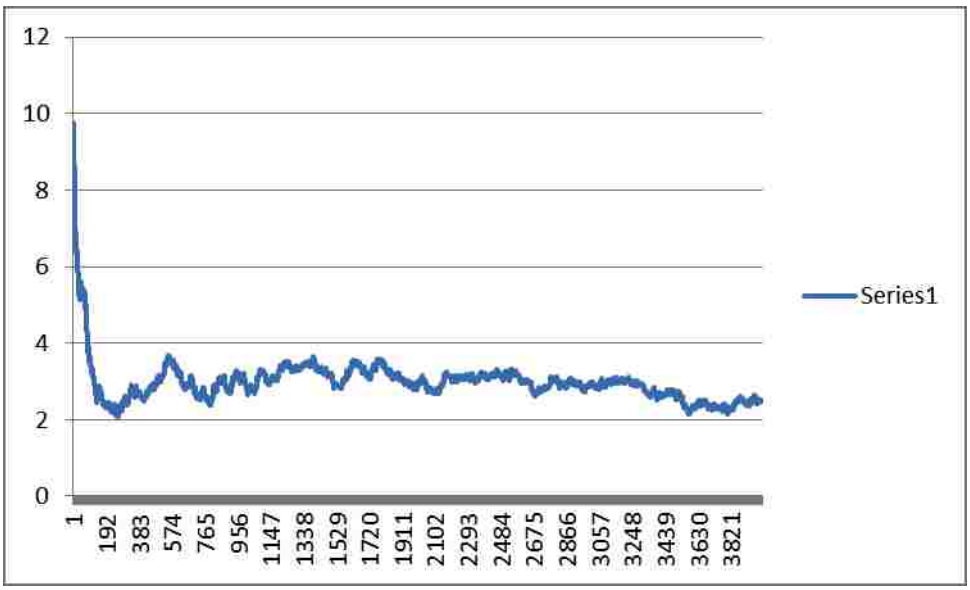

Figure 5 (b) the distance between the center of the polymer chain and the wall Rz versus time-steps in the case that z_{ini} =10 and ε_{wall} =3 in the quiescent state.

It should also be noted that the initial distance between the polymer chain and the wall z_{ini} has a dramatic effect on the R_g. When $\varepsilon_{wall} > 1$, as shown in Figure

4(a) and 4(b), the larger z_{ini} is, the smaller R_g becomes. As expected the wall has a stronger impact on the stretch of the polymer chain after first phase, considering when the polymer chain is closer to the wall.

For the case of a quiescent Solvent, the wall energy parameter ε_{wall} is varied from 0.1 to 10 gradually in order to simulate the weakly attractive and the strongly attractive walls. In Figures 4(a) and (b), for the weakly attractive wall (ε_{wall} is smaller than 1), R_g is comparatively small and nearly constant at 1.755. For the values of ε_{wall} near unity, R_g decreases slightly from 1.755 to about 1.7. For strongly attractive wall (ε_{wall} is greater than 1), R_g increases rapidly. The transition occurs since the forces that the Lennard-Jones wall exerts on polymer beads change from repulsive to attractive and the polymer chain sticks to the wall rather than it is pushed away. When this happens, the chain unfolds as displayed on Figures 6(a) and (b). After the transition section, the R_g is nearly stable if neglecting little fluctuation.

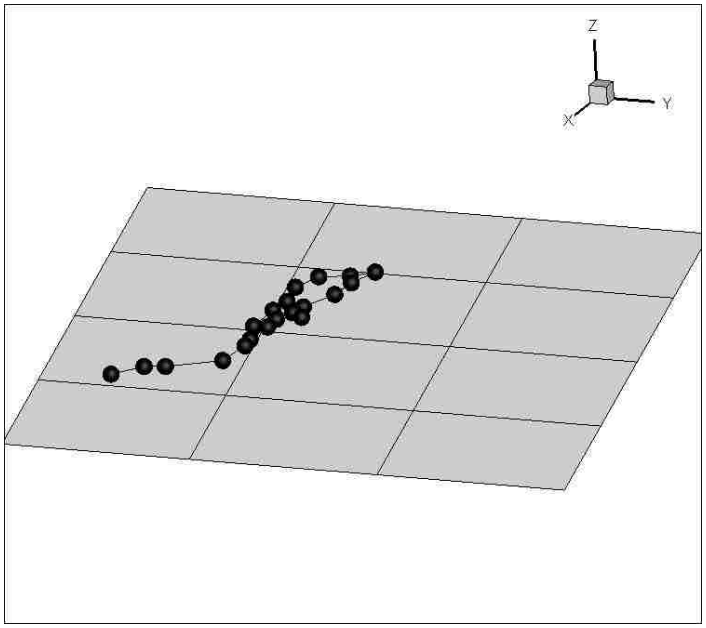

Figure 6 (a) Schematic representation of a single polymer chain confined by a solid wall (infinite) after enough time-steps that the single polymer chain sticks to the wall.

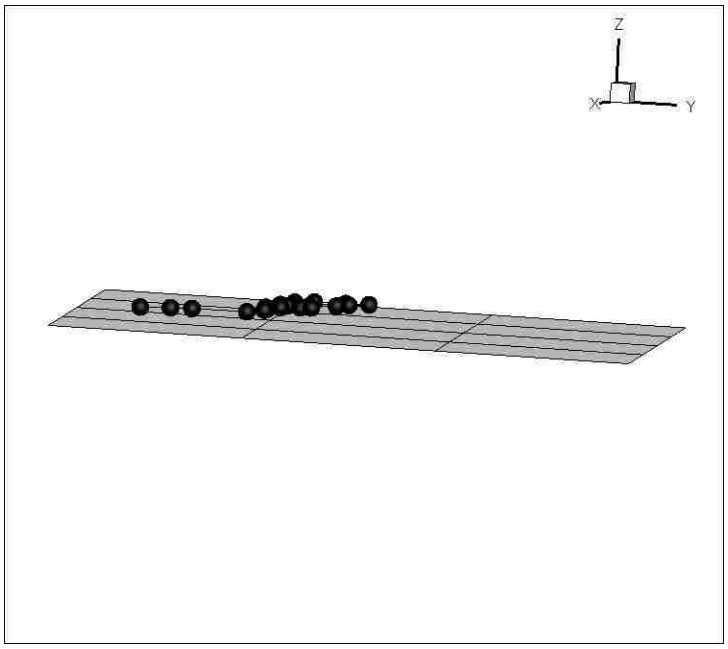

Figure 6 (b) Schematic representation of a single polymer chain confined by a solid wall (infinite) after enough time-steps that the single polymer chain sticks to the wall.

5.2 The polymer chain in flow

Next, the dynamics of a polymer chain in flow is probed. The polymer chain is subjected to a simple shear flow. The intensity of the simple shear flow is characterized by the gradient of the velocity

$$\nabla \mathbf{u}^T = \begin{pmatrix} 0 & 0 & \dot{\gamma} \\ 0 & 0 & 0 \\ 0 & 0 & 0 \end{pmatrix} \tag{19}$$

Where $\dot{\gamma}$ is the shear-rate, namely $\dot{\gamma} = \frac{\partial u}{\partial z}$. And the flow in the simulations is in the x-direction (direction parallel to the wall). The shearing is in z-direction (direction normal to the wall). The intensity of the shear flow is characterized in terms of Weissenberg number, $Wi = \tau\dot{\gamma}$, where τ is the longest relaxation time of a polymer chain that we have discussed in the Chapter 4.

Figure 7(a) and (b) display the radius of gyration (R_g) of the 20 bead polymer chain as a function of the wall energy parameter under various values of Weissenberg (Wi) Number as z_{ini} is fixed at 20. For all cases, as the intensity of shearing increases the polymer unfolds more for any type of walls (weakly attractive or strongly attractive walls). It should be noted that the conformation changes of polymer in shear flow is very different compared to that of the polymer chain in quiescent solvent. For weakly attractive wall (ε_{wall} is smaller than 1), R_g changes rapidly as ε_{wall} approaches to unity. R_g assumes a minimum

value at $\varepsilon_{wall} = 1$ and it increases as ε_{wall} increases from unity as depicted in Figure 7(a) and 7(b).

Unlike for the no flow case, the polymer chain experience a transition when ε_{wall} approaches to unity from the weakly attractive wall. During such transition the polymer folds rapidly. At the other side of unity of ε_{wall}, the unfolding transition is weaker compared to the one for folding transition. For both in flow and in quiescent cases, the polymer chain interacts with the wall stronger when ε_{wall} is near unity.

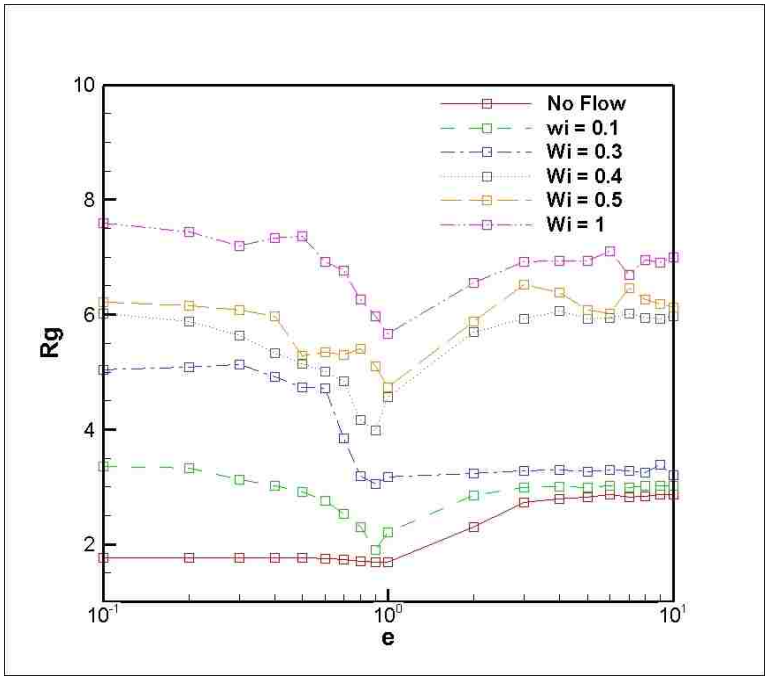

Figure 7 (a) Dependence of the radius-of-gyration R_g for a 20-bead chain on energy parameter of bead-wall interactions ε_{wall} in cases when Wi equals 0, 0.1, 0.3, 0.5 and 1.

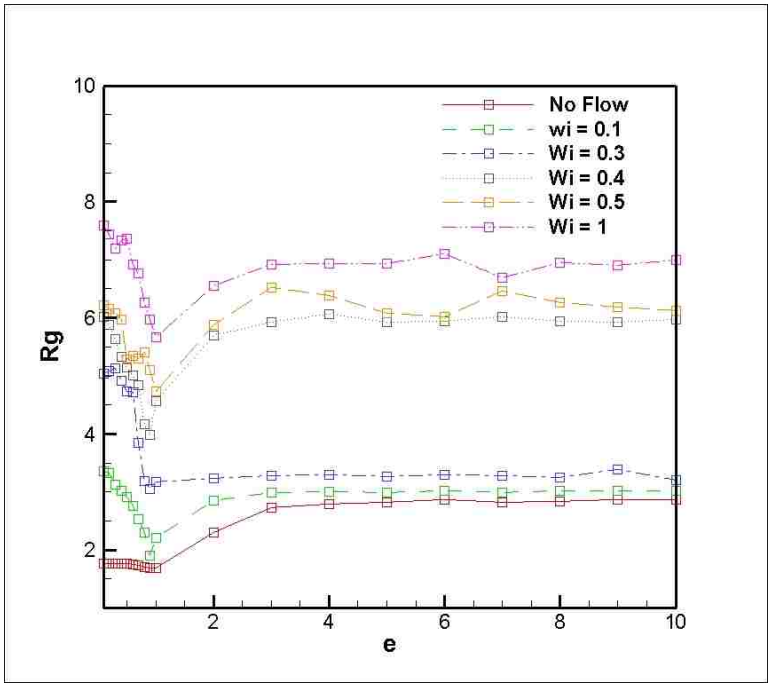

Figure 7 (b) Dependence of the radius-of-gyration R_g for a 20-bead chain on energy parameter of bead-wall interactions ε_{wall} in cases when Wi equals 0, 0.1, 0.3, 0.5 and 1. And the value of ε_{wall} is using log scale.

It is obvious from Figure 7(a) and (b) that there is a critical value of Wi, below which the polymer chain near a strongly attractive wall (ε_{wall} is greater than 1) unfolds very slightly compared to that of the polymer chain in quiescent solvent. For the shearing above the critical value of the Wi is predicted to be 0.4, as seen in Figure 7(a) and (b). This critical phenomenon is not obvious when the wall is weakly attractive. The polymer chain near the weakly attractive wall experiences the unfolding even under weak shear flow conditions.

The transition in the conformational changes of the polymer chain in shear flow conditions and the effects of weakly and strongly attractive walls are clearly seen in Figure 8(a) ~ 8(l).

The value of the radius of gyration (R_g) as a function of time is plotted in Figure 8(a) ~ 8(l) for various flow conditions and various types of walls.

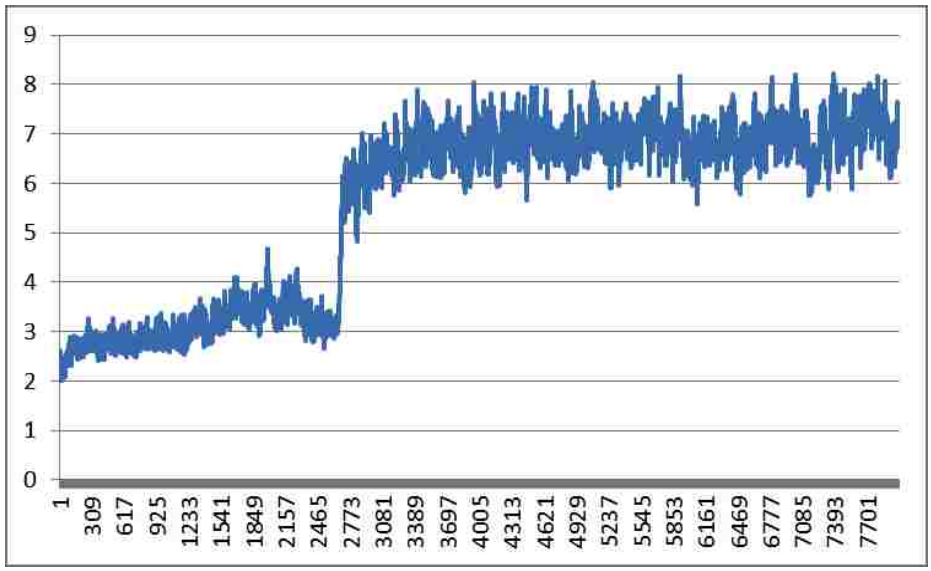

Figure 8 (a) The radius of gyration R_g versus time-steps when Wi equals 1 and ε_{wall} equals 5.

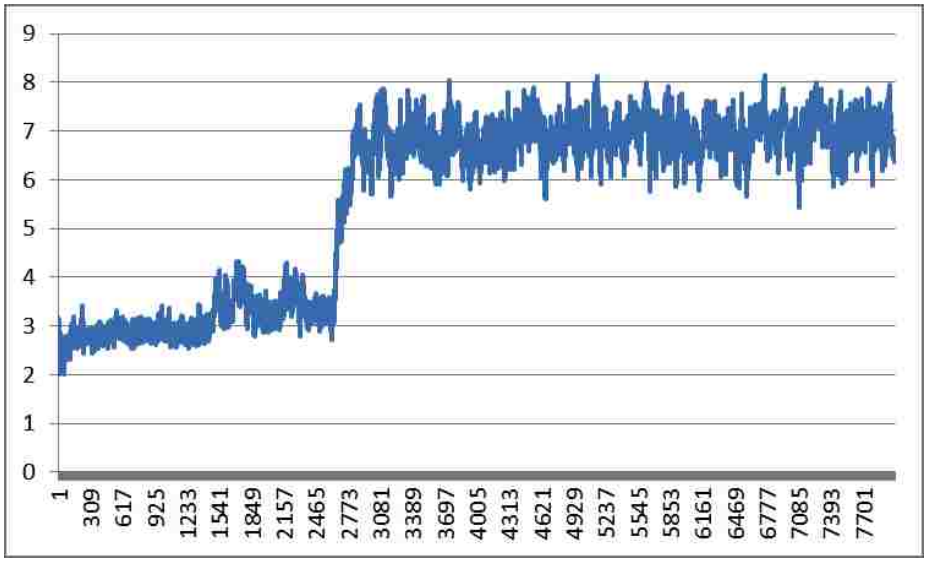

Figure 8 (b) The radius of gyration R_g versus time-steps when Wi equals 1 and ε_{wall} equals 9.

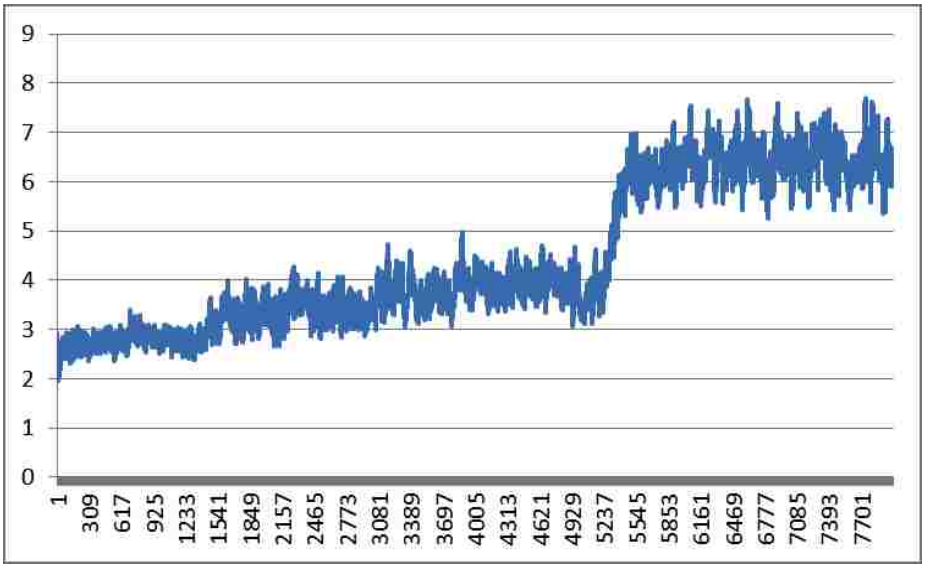

Figure 8 (c) The radius of gyration R_g versus time-steps when Wi equals 0.5 and ε_{wall} equals 5.

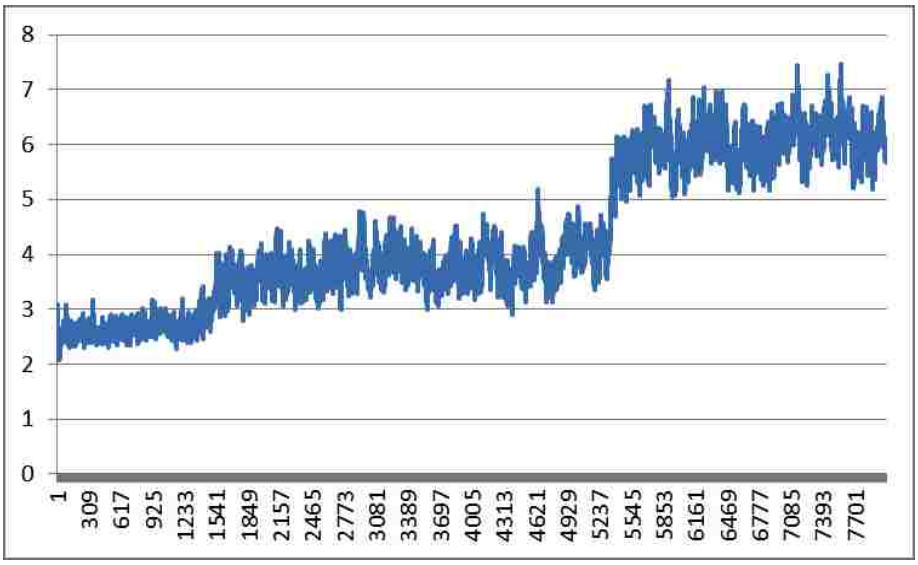

Figure 8 (d) The radius of gyration R_g versus time-steps when Wi equals 0.5 and ε_{wall} equals 9.

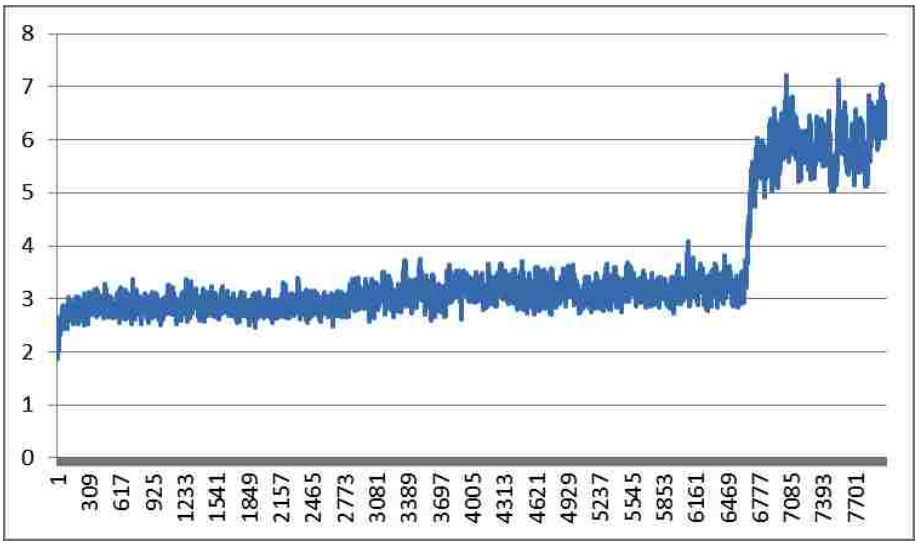

Figure 8 (e) The radius of gyration R_g versus time-steps when Wi equals 0.4 and ε_{wall} equals 5.

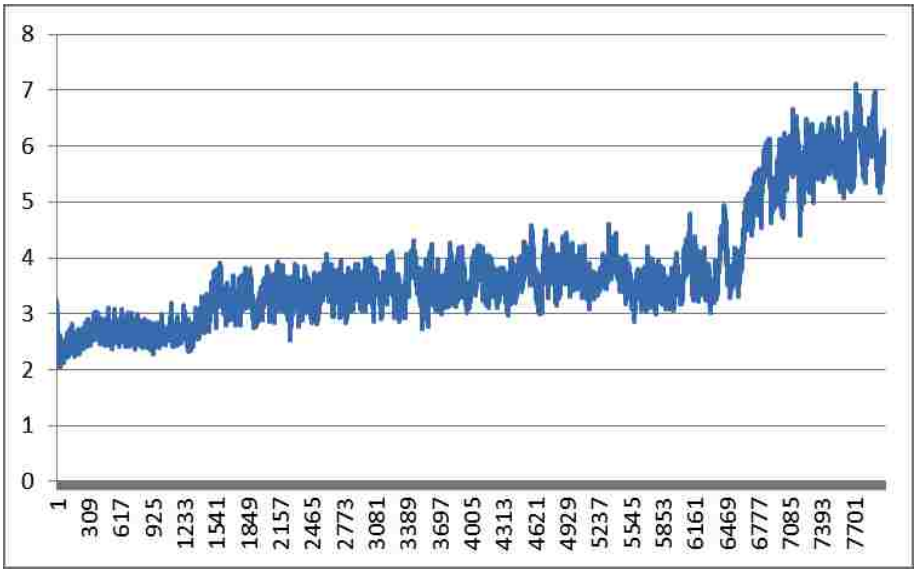

Figure 8 (f) The radius of gyration R_g versus time-steps when Wi equals 0.4 and ε_{wall} equals 9.

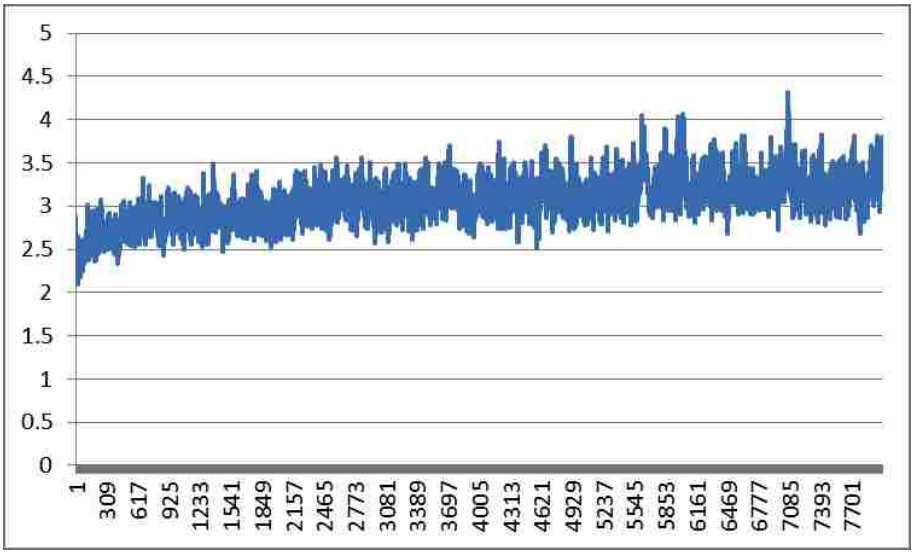

Figure 8 (g) The radius of gyration R_g versus time-steps when Wi equals 0.3 and ε_{wall} equals 5.

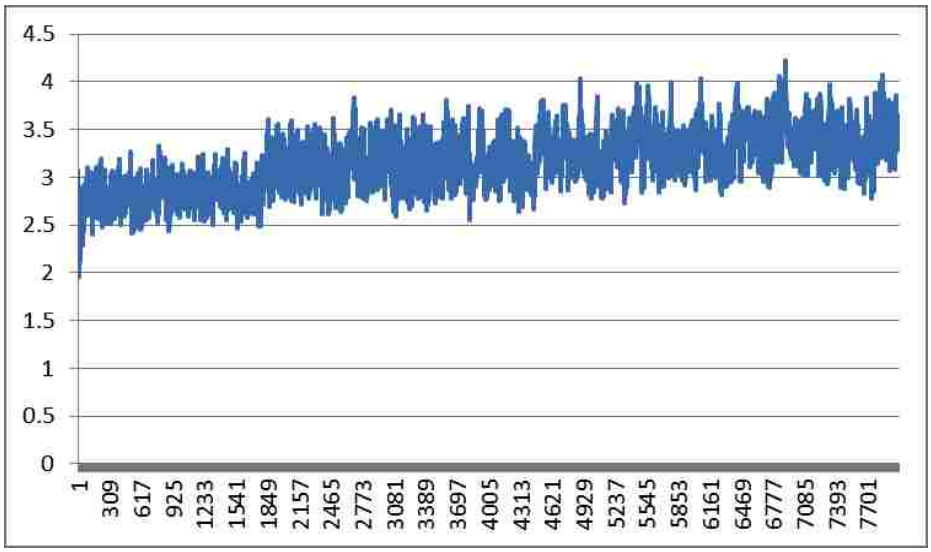

Figure 8 (h) The radius of gyration R_g versus time-steps when Wi equals 0.3 and ε_{wall} equals 9.

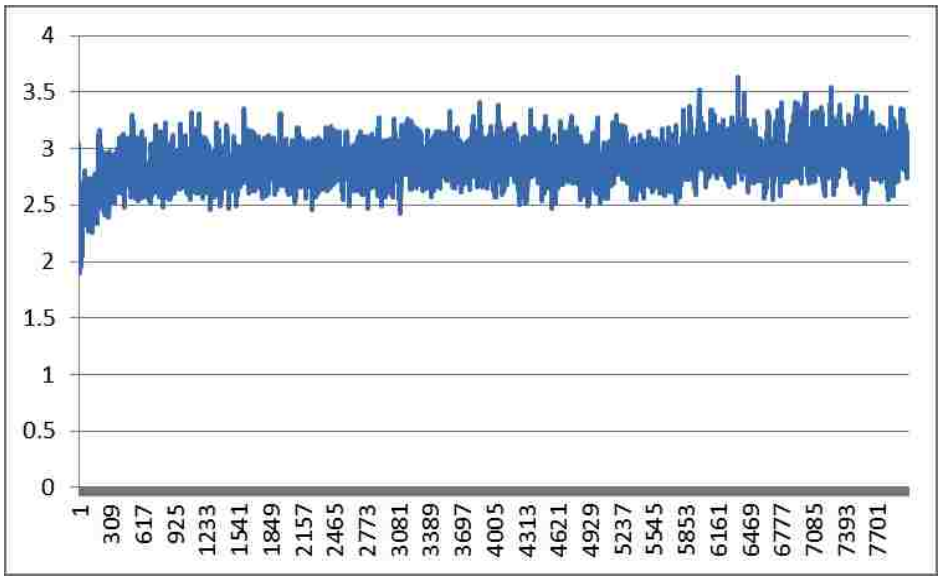

Figure 8 (i) The radius of gyration R_g versus time-steps when Wi equals 0.1 and ε_{wall} equals 5.

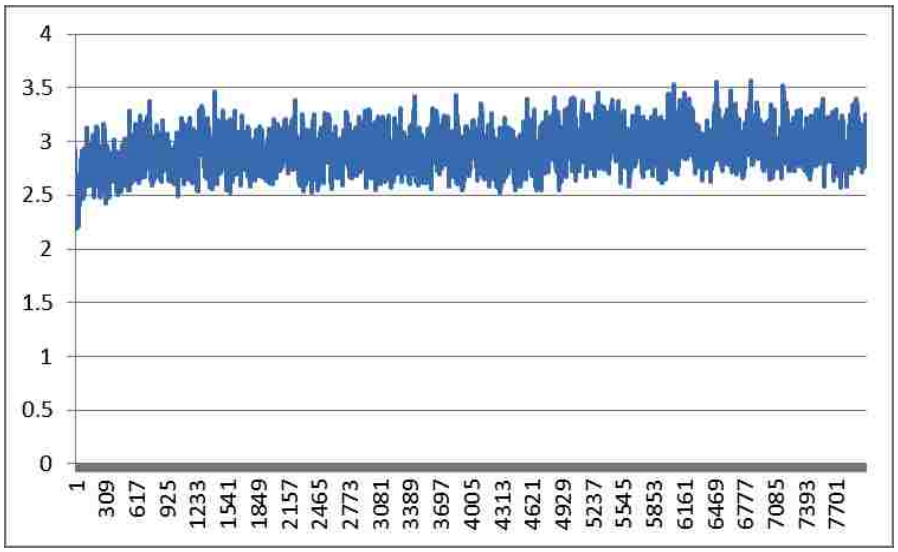

Figure 8 (j) The radius of gyration R_g versus time-steps when Wi equals 0.1 and ε_{wall} equals 9.

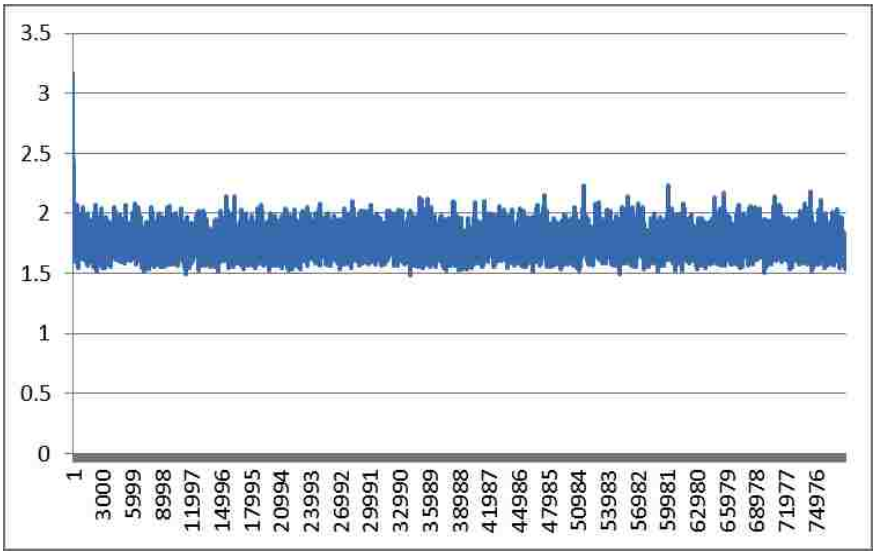

Figure 8 (k) The radius of gyration R_g versus time-steps when Wi equals 0 and ε_{wall} equals 5.

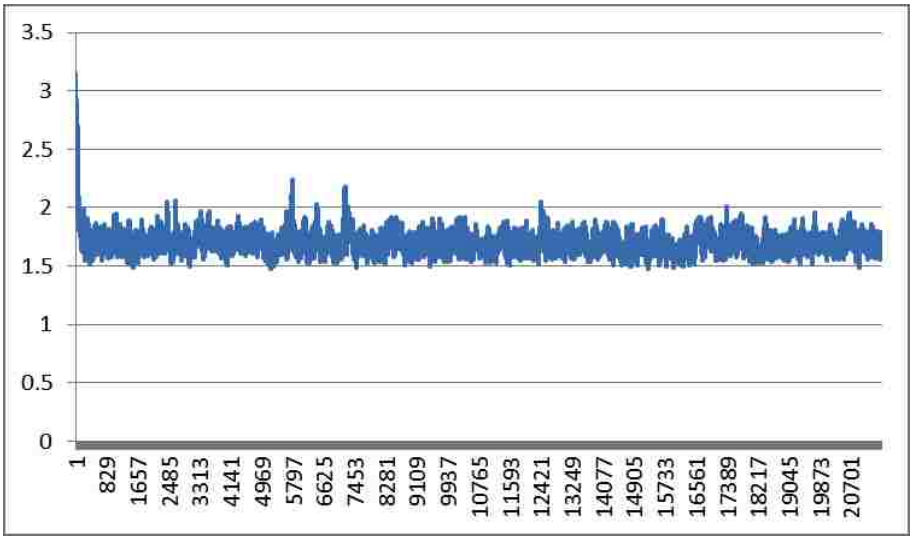

Figure 8 (l) The radius of gyration R_g versus time-steps when Wi equals 0 and ε_{wall} equals 9.

Chapter 6. Conclusion

Coarse-grained molecular dynamics simulations are conducted to investigate the effect of wall on the conformational changes of a single polymer chain near wall. The polymer chain is subject to shear flow. Both transient and long-time dynamics of the polymer are studied. Both weakly and strongly attractive walls are considered in the present work.

For a polymer chain in quiescent solvent, the effect of the wall on the dynamics of the polymer is minimal. The polymer drifts away from the wall and the wall-bead LB potential forces becomes too small to influence the conformation of the chain. As the wall becomes more attractive, the polymer chain sticks to the wall and unfolds rapidly.

The polymer chain near the wall under shear flows unfolds for any type of walls: weakly or strongly attractive ones. The effect of the wall under flow is very different compared to that in quiescent solvent. The polymer chain near weakly attractive wall unfolds. The extent of unfolding is greatly reduced as ε_{wall} tends to unity. The wall with energy coefficient $\varepsilon_{wall} = 1$ causes least degree of unfolding of the chain under flow or no flow conditions.

There is a critical value of shear rate, above which the polymer chain starts unfolding when the wall is strongly attractive. Such transitional behavior is weak or not present for the polymer chain near weakly attractive wall.

BIBLIOGRAPHY

[1] Emmanouil Glynos, Alexandros Chremos, *Polymer-like to Soft Colloid-like Behavior of Regular Star Polymers Adsorbed on Surfaces*, Macromolecules 2007, 40, 6947-6958.

[2] Sean P. Holleran, Ronald G. Larson, *Using spring repulsions to model entanglement interactions in Brownian dynamics simulations of bead-spring chains*, Rheol Acta 2008, 47, 3-17.

[3] Nazish Hoda, Ronald G. Larson, Brownian dynamics simulations of single polymer chains with and without self-entanglements in theta and good solvents under imposed flow fields, J. Rheol 2010, 54(5), 1061-1081.

[4] IUPAC Compendium of Chemical Terminology, 2nd Edition, 1997.

[5] Prince E. Rouse, A Theory of the linear Viscoelastic Properties of Dilute Solutions of Coiling Polymers, J. Chem. Phys 1953, 21, 1272.

[6] Tony W. Liu, Flexible polymer chain dynamics and rheoligical properties in steady flows, J. Chem. Phys 1989, 90, 5826.

[7] Bruno H. Zimm, Dynamics of Polymer Molecules in Dilute Solution: Viscoelasticity, Flow Birefringence and Dielectric Loss, J. Chem. Phys 1956, 24, 269.

[8] Harold R. Warner, Kinetic Theory and Rheology of Dilute Suspensions of Finitely Extendible Dumbbells, Ind. Eng. Chem. Fundamen 1972, 11(3), 379-387

[9] Robert C. Armstrong, Kinetic theory and rtheology of dilute solutions of flexible macromolecules, J. Chem. Phys. 1974, 60, 724.

[10] Richard L. Christiansen, R. Byron Bird, Dilute solution rheology: experimental results and finitely extensible nonlinear elastic dumbbell theory, J. Non-Newtonian Fluid Mech 1977, 3, 161-177.

[11] X. J. Fan, R. Byron Bird, Configuration-dependent friction coefficients and elastic dumbbell rheology, J. Non-Newtonian Fluid Mech 1985, 18, 255-272.

[12] Bird, R. B., C. F. Curtiss, R. C. Armstrong, and O. Hassager, Dynamics of Polymeric Liquids, Vol. 2.

[13] D. L. Ermak, J. A. McCammon, Brownian dynamics with hydrodynamic interactions, J. Chem. Phys 1978, 69, 1352.

[14] M. Fixman, Brownian dynamics of chain polymers, Faraday Discuss. Chem. Soc. 1987, 83, 199-211.

[15] J. W. Rudisill, P. T. Cummings, Brownian dynamics simulation of model polymer fluids in shear flow. I. Dumbbell models, J. Non-Newtonian Fluid Mech 1992, 40, 275-288.

[16] B.H.A.A. VandenBrule, Browian dynamics simulation of finitely extensible bead-spring chains, J. Non-Newtonian Fluid Mech 1993, 47, 357-378.

[17] J. S. Hur, R. G. Larson, Brownian dynamics simulations of single DNA molecules in shear flow, J. Rheol 2000, 44, 713.

[18] M. Chopra, R. G. Larson, Brownian dynamics simulations of isolated polymer molecules in shear flow near adsorbing and nonadsorbing surfaces, J. Rheol 2002, 46, 831.

[19] V. G. Mavrantzas, A. N. Beris, Modeling and Simulation of the Dilute Polymer Solution Flow behavior Next to Solid Surfaces and Interfaces, Polymer Preprints(USA) 1992, 33, 615-616.

[20] De Gennes P. G., Some conformation problems for long macromolecules, Rep. Prog. Phys. 1969, 32, 187.

[21] De Gennes P. G. Scaling Concepts in Polymer Physics, Cornell University Press 1979.

[22] J. M. H. M. Sheutjens, G. J. Fleer, Statistical theory of the adsorption of interacting chain molecules, J. phys. Chem. 1979, 83, 1619-1635.

[23] H. J. Ploehn, W. B. Russel, C. K. Hall, Self-consistent field model of polymer adsorption: generalized formation and ground-state solution, Macromolecules 1988, 21, 1075-1085.

[24] J. H. Aubert, M. Tirrell, Effective viscosity of dilute polymer solutions near confining boundaries, J. Chem. Phys 1982, 77, 553.

[25] P. O Brunn, Wall effects for Dilute Polymer Solutions in Arbitrary Unidirectional Flows, J. Rheol 1985, 29, 859.

[26] E. Duering, Y. Rabin, Polymers in shear flow near repulsive boundaries, Macromolecules 1990, 23, 2232-2237.

[27] De Pablo, Y. Rabin, Hydrodynamic changes of the depletion layer of dilute polymer solutions near a wall, AIChE Journal 1992, 38, 273-283.

[28] V. G. Mavrantzas, A. N. Beris, A hierarchical model for surface effects on chain conformation and rheology of polymer solutions, J. Chem. Phys. 1999, 110, 628.

[29] S. W. Sides, G. S. Grest, Surface-tethered chains entangled in a polymer melt: Effects on adhesion dynamics, Phys. Rev. E 2001, 64, 050802(R).

[30] S. W. Sides, G. S. Grest, Effect of End-Tethered Polymers on Surface Adhesion of Glassy Polymers, J. Polymer Science 2004, 42, 199-208.

[31] Larson, R. G., The structure and Rheology of Complex Fluids, Oxford University Press 1999.

[32] N. Hoda, R. G. Larson, Brownian dynamics simulations of single polymer chains with and without self-entanglements in the theta and good solvents under imposed flow fields, J. Rheol 2010, 54, 1061-1081.

Vita

Wenli Ouyang was born in Jinzhou, China on 12 January, 1988, the son of Ming Ouyang and Ailin Hu. His preliminary education was in his home town. He earned his bachelor's Degree in Mechanical Engineering from Hua Zhong University of science and technology in June 2010. Afterwards he entered The Graduate School at Lehigh University, USA, to pursue his Master of Science degree. He also participated in the Lehigh University's Industrial Assessment Center program.